# Accepted Manuscript

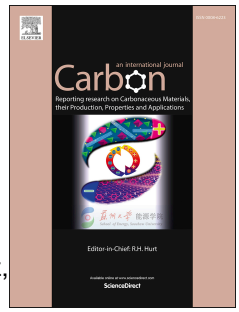


Determinant influence of the electrical conductivity versus surface area on the performance of graphene oxide-doped carbon xerogel supercapacitors

Gloria Ramos-Fernández, María Canal-Rodríguez, Ana Arenillas, J. Angel Menéndez, Iluminada Rodríguez-Pastor, Ignacio Martin-Gullon

PII: S0008-6223(17)31019-9

DOI: 10.1016/j.carbon.2017.10.025

Reference: CARBON 12462

To appear in: *Carbon*

Received Date: 27 March 2017

Revised Date: 5 October 2017

Accepted Date: 8 October 2017

Please cite this article as: G. Ramos-Fernández, Marí. Canal-Rodríguez, A. Arenillas, J.A. Menéndez, I. Rodríguez-Pastor, I. Martin-Gullon, Determinant influence of the electrical conductivity versus surface area on the performance of graphene oxide-doped carbon xerogel supercapacitors, *Carbon* (2017), doi: 10.1016/j.carbon.2017.10.025.

*Factors influencing the performance of mesoporous carbon xerogel EDLC capacitors*

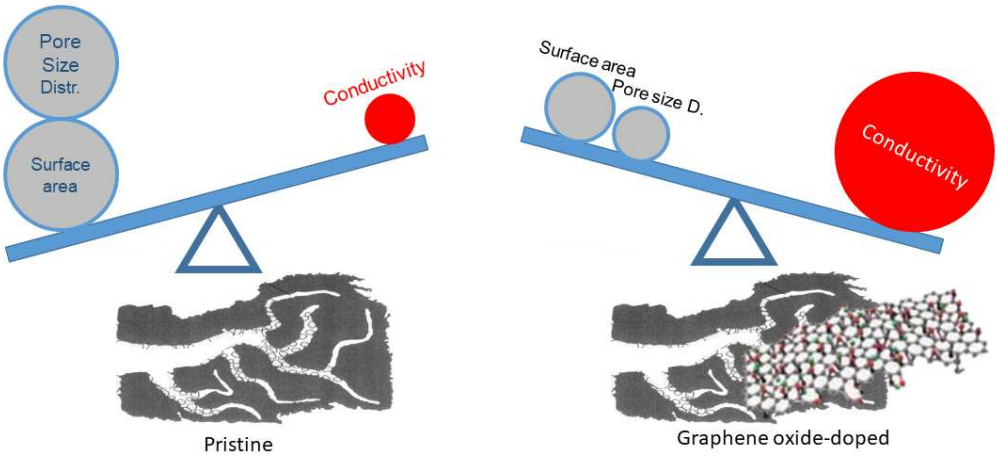

# Determinant influence of the electrical conductivity versus surface area on the performance of graphene oxide-doped carbon xerogel supercapacitors.

Gloria Ramos-Fernández[(1)], María Canal-Rodríguez[(2)], Ana Arenillas[(2)], J. Angel Menéndez[(2)], Iluminada Rodríguez-Pastor[(1)], Ignacio Martin-Gullon[*(1)]

(1) Chemical Engineering Dept, University of Alicante, Apartado 99, 03080 Alicante, Spain

(2) Instituto Nacional del Carbón, CSIC, Apartado 73, 33080 Oviedo, Spain

## Abstract

A series of resorcinol formaldehyde based carbon xerogels were synthesized under identical conditions using different graphene oxide loads. The gelification reaction was carried out using a stable aqueous suspension of graphene oxide, yielding organic gels with graphene oxide concentrations ranging from 1.2 to 2.5%. After the carbonization, xerogels with medium surface area (650 $m^2/g$) and a highly improved electrical conductivity were obtained. Specific capacitance of 120 F/g of one electrode at very high scan rate of 500 mV/s were achieved, as well as power densities above 30 kW/kg, which is a significant improvement of 180% with respect to the pristine xerogels. Carbonized xerogels were further steam activated to yield activated carbon xerogels with surface areas of up to 1800 $m^2/g$. The use of activated xerogels improves slightly the specific capacitance at low scan rates only, and there is a sharp decrease above 20 mV/s, resulting in a worse performance than graphene oxide doped carbonized xerogels. The electrical conductivity of the graphene oxide-doped carbon xerogels decreases upon activation, which means that the influence of the electrical conductivity on a carbon xerogel is greater than its specific surface area, which it is is the first time it is observed for porous carbons.

[*] Corresponding author. Tel: +34-965903867. Email: gullon@ua.es

## 1. Introduction

Electrochemical energy storage devices, such as supercapacitors (SCs), batteries and fuel cells have attracted widespread attention among the scientific community over the last few decades due to the increasing use of renewable energy and the rapid growth in demand for electricity by electronic goods and electric vehicles. Electrical double layer capacitors (EDLC), based on the physical accumulation of the charge by means of electrolyte species over an accessible surface, show an excellent cyclability, low maintenance and a longer life span and a safer operation record than pseudo-capacitive SCs, whose energy storage mechanism is based on redox chemical reactions [1-3]. Electrode materials are one of the most important factors for the improvement of the electrochemical performance of EDLCs, to get a higher energy storage capacity and power densities. EDLCs are based on high surface area carbon based materials, mainly porous carbons such as biomass or coal derived activated carbons [4, 5].

The energy storage capacity of SCs is theoretically independent of the voltage and depends mainly on the available area, which is determined as the part of the total specific area corresponding to the porosity accessible to the electrolyte. Carbon materials are suitable due to their i) high conductivity, ii) high surface area (even above 2000 $m^2/g$), iii) good resistance to corrosion and thermal stability, iv) controlled pore structure, v) good processability and vi) relatively low cost [6]. Literature shows clear evidence of a better performance in relation to specific capacitance when BET surface area is increased, taking into account that the surface area must be accessible to the electrolyte. Then parameters such as average pore size, effective ion size and the pore size distribution in the carbon materials play also an important role [7]. On the other hand, Kötz and Carlen [8] claim that the electrical conductivity of the carbon materials must simply be greater than that of the electrolyte, which means that it is more effective to have a large number of short micropores than to have less deep or tortuous micropores. Consequently, most efforts are focused on developing a very high surface area with tuned pore sizes, to allow the highest possible amount of electrolyte to be stored and the fastest possible kinetic adsorption-desorption mechanism capability.

Activated carbons with a very high BET surface area can show a high specific capacitance at low scan (or current) rates, but capacitance normally decreases at higher rates due to the slow kinetics caused by a heterogeneous pore size distribution. The use

of carbon nanomaterials such as carbon nanotubes [9] [10], carbons onions [11], and high porosity derived graphene [12], show more stable energy densities when the scan rate is increased, but not such a high specific capacity justifies a huge cost. Another option is to develop synthetic porous carbons such as zeolite-templated carbons [10], carbide-derived carbons [13, 14] or carbon derived from sol-gel materials [15, 16]. These perform better due to their larger surface area and the fact that their pore size distribution can be tuned, yielding capacitances of 150-200 F/g at a reasonable cost in the case of the sol-gels, although their power densities are still low [17].

Carbon gel materials, like carbon aerogel, cryogel and xerogel, based on resorcinol (R) and formaldehyde (F), offer a greater potential [15, 18, 19] than the traditional activated carbons due to their (i) low electrical resistivity; (ii) high purity; (iii) the ability to develop the desired pore texture and pore size distributions through a control of the synthesis conditions [20]; (iv) their different morphologies (monolith, powder, spheres…). However, they also show a limited energy capacity and power density when the current density is increased like other porous carbons. Power density is inversely proportional to the equivalent series resistance (ESR), which is related to the electrical conductivity although its quantitative influence with respect to other factors like the BET surface area is not yet clear. In view of these problems, modifications methods of carbon xerogel have been suggested [21] in order to control the effect of the synthesis preparations conditions, such as modifying the pH, R/F molar ratio, gelation time, temperature, dilution factor, drying conditions and carbonization conditions. Other modifications include the synthesis of boron, nitrogen [22] and sulfur doped carbon gels to modify their surface chemistry and wettability [23]. In any case, carbon gels must necessarily be activated in an oxidative atmosphere to maximize the BET surface area to attain the required energy densities. Furthermore, hybrid EDLCs based on carbon xerogel composites with carbon nanomaterials, like carbon nanotubes (CNT) [24, 25] and graphene related materials have been studied, since theoretically graphene could achieve a capacitance of ~540 F/g, if all the surface area of the graphene layers could be used [26]. To promote a good dispersion and avoid aggregation, graphene oxide (GO) is an excellent choice for the preparation of composite carbon materials, since GO has functional groups in the sheet basal plane and at the edges [27], which facilitate their dispersion in aqueous media, and the formation of sol-gel using GO sheets (which contain hydroxyl and phenol groups) as scaffold. Lee et. al [28] prepared composite

materials synthesizing RF gel in the presence of GO functionalized with polyethyleneimine (PEI), using an unspecified load, and compared the subsequent activated aerogel with the pristine one. The resulting GO doped activated aerogel attained 1158 $m^2/g$ (versus 1384 $m^2/g$ the pristine aerogel) and a specific capacitance, as measured by cyclic voltammetry (CV), of 221 F/g at 10 mV/s and 141 F/g at 200 mV/g in an aqueous medium, which is an excellent result despite a reduction of 37% with an increase in the scan rate. The pristine aerogel performed around 23% less well with a similar reduction with the scan rate. The better performance of the GO aerogels, that had a slightly lower BET specific surface area, was attributed to its lower ESR. Qian et al. [29] reported a similar decrease in performance with an increase in current flux when working with GO and resol phenolic resin. In short, a lower ESR, which is related to electric conductivity, is obtained with GO and a synthetic carbon as a matrix, yielding higher specific capacitances at slightly lower BET surface areas, although there is still a considerable decrease in its performance with an increase of the scan rate.

The challenge of RF carbon based gels is to attain stable capacitances at high rates, and to achieve this a low ESR seems to be required. The objective of this work is to produce GO-carbon xerogel composites with a tailored electrical conductivity and porosity by varying the load of GO and the activation burn-off, in order to produce carbon materials with stable capacitances, even at high rates. Carbonized carbon xerogels were produced using the same gelification conditions with three different graphene oxide concentrations, and a pristine carbonized xerogel for comparison purposes. The RF gelation was carried out in the presence of graphene oxide, dispersed in water. During the carbonization of the organic xerogel, the graphene oxide sheets were converted into reduced graphene oxide (rGO), and this was embedded in the carbon xerogel matrix. In order to increase the electrical conductivity of the carbon xerogels, a minimum amount of GO was required to attain the electric percolation point. Subsequently, the carbonized xerogels were steam activated at two burn-off degrees. The results corresponding to the carbonization and activation mass yields, specific surface area, electrical conductivity, CVs from 1 mV/s to 500 mV/s and galvanostatic charge-discharge cycles were analyzed.

## 2. Experimental

### *1.1. Graphene Oxide preparation*

GO was synthesized from a commercially natural expanded graphite powder (BNB 90, Timcal) using the modified Hummers-Offemann method [30]. Basically, 1 g of graphite was mixed and stirred at room temperature with 150 mL of $H_2SO_4$ (95%, sigma Aldrich) and 1 g of $NaNO_3$ (Sigma Aldrich). After 3 h, 4 g of $KMnO_4$ were added and stirred for an additional 2 h. When the reaction was completed, it was poured into around 400 g of ice cubes with 20 mL of $H_2O_2$ (33vol. 33%, VWR international). After several rinses of diluted HCl 0.1 N and water, the remaining solid product (graphite oxide) was dried overnight at 70 °C. The oxidized solid was subsequently suspended in water at different concentrations (ranging from 10 mg/mL to 20 mg/mL) and exfoliated by high-energy tip sonication (QSonica Ultrasonic Q500) at 30 W for 2 h, in periods of 60s ON and 30s OFF to produce GO.

*2.2. Synthesis of Carbon Xerogel*

Initially an organic gel was synthesized by the polycondensation of resorcinol (Sigma Aldrich) with formaldehyde (37 wt-% water and 10-15 wt-% methanol, VWR International) in water as a solvent and with sodium carbonate as gelation catalyst, based on the method described by Pekala et al.[31]. The present work carries out the synthesis of the organic gel by substituting an aqueous suspension of GO at different concentrations (10, 15, 20 mg/mL) by the water. Thus, the gel is formed using a GO sheet as a scaffold platform. A GO-free organic gel was also synthesized for comparison purposes.

All the organic gels were synthesized at a resorcinol/catalyst (R/C) molar ratio of 750, a R/F molar ratio fixed to a stoichiometric value of 0.5, and a dilution ratio (i.e. a total solvent/reactant molar ratio), of 5.7. Resorcinol and sodium carbonate, as catalyst for the adjustment of pH, were dissolved first in the graphene oxide aqueous suspension under magnetic stirring, and then the formaldehyde solution was added. As GO suspensions have a high acidic pH, concentrated NaOH was used to correct and fix an starting pH of 6.4, which corresponds to the initial pH when producing the pristine gel. Experimental details of the gelation, drying, pyrolysis and activation are provided in the supplementary data (SD). Breafly, gelation was performed at 85°C for 72 hours. Drying was carried out using a vacuum controlled program up to 150°C and down to -1 bar. The resulting GO loads in the precursor organic xerogel composites are 1.2, 1.9 and 2.5 wt-% corresponding to the GO concentrations of 10, 15 and 20 mg/mL in the initial

water suspensions, respectively. The organic xerogels were carbonized at a final temperature of 800°C, and the samples were denoted by the label CX followed by the GO concentration present in the initial organic gel, since an accurate quantification of the final GO content of the doped samples was not possible. The carbonization yield was then recorded. The carbonized xerogels were steam activated at 800°C for 10 minutes and 60 minutes, and burn-off was also adequately recorded. The nomenclature of the activated samples was ACX-μ-β, where μ represents the GO content of the original organic-xerogel and β the duration of the activation process.

*2.3 Textural characterization of the carbon xerogel*

The textural properties of the carbon xerogels were evaluated from 77K $N_2$ adsorption-desorption isotherm and 273K $CO_2$ adsorption isotherm, by means of Quadrasorb-Kr/MP (Quantachrome Instruments) equipment. The specific surface area, $S_{BET}$, was calculated by applying BET [32] equation to the 77K $N_2$ adsorption isotherm data in the relative pressure range of 0.05-0.10. The micropore volume ($V_{micro}$) was calculated by applying the Dubinin-Raduskevich (DR) equation [33] to the nitrogen adsorption isotherm, and the total pore volume ($V_p$) was calculated from the amount of nitrogen adsorbed at saturation point. The average micropore size was estimated by applying the Dubinin and Stoeckli equation using the DR adsorption energy [34].

The morphology of the xerogels was studied by transmission electron microscopy TEM (JEOL, JEM-2010) and field emission scanning electron microscopy FE-SEM (ZEISS, Merlin VO Compact). The samples were dispersed in 2-propanol, sonicated and deposited on a carbon-coated copper grid.

*2.4 Electric and electrochemical characterizations*

The preparation of the electrodes was performed following the same procedure in all cases, as explained in the SD. Analysis of the electrochemical behavior of the materials under study was carried out at room temperature, using 1M $H_2SO_4$ as electrolyte, and applying cyclic voltammetry (CVs) and constant charge-discharge (CD) current by means of BT-G-502 4CH ARBIN potentiostat. The CVs were applied out in a voltage window of between 0 and 1.0 V at different scan rates (1, 2, 5, 10, 20, 50,100, 200, 500 mV/s) in order to detect possible pseudocapacitive contributions and assess the charge storage capacity of the device. The CD measurements were performed at different

current densities (0.1, 0.2, 0.5, 0.6, 0.8, 1.0 A/g) with a potential fixed at 1V, to evaluate the specific capacitance. On the other hand, selective samples were characterized by electrochemical impedance spectroscopy (EIS), by means a potentiostat/galvanostat VMP Biologic. EIS analysis was done at open-circuit voltage (0 V) within the frequency range of 1 mHz–100 kHz and 10 mV AC amplitude.

The electrical conductivity of the electrodes was determined by the van der Pauw method [35]. For this purpose an apparatus based on that designed by Euler [36] and used by Celzard et. al [37] for the measurement of electrical conductivity of carbon black was employed.

## 3. Results and discussion

Figure 1 shows the carbon xerogel weight yields obtained for both non-activated and activated samples during 10 and 60 minutes. After the carbonization, there is a practically constant yield for pristine and graphene doped carbons, of around 58 wt-%. However, 10 minutes of steam activation decreases the yield in a higher extent for GO-xerogel composites to around 45 wt-%, compared to above 50 wt-% for pristine carbon xerogel, indicating that GO-carbon xerogel composites are slightly more reactive when subjected to steam activation. 60 minutes of activation time produces more marked differences among GO doped xerogels, with CX-1.9 showing highest reactivity.

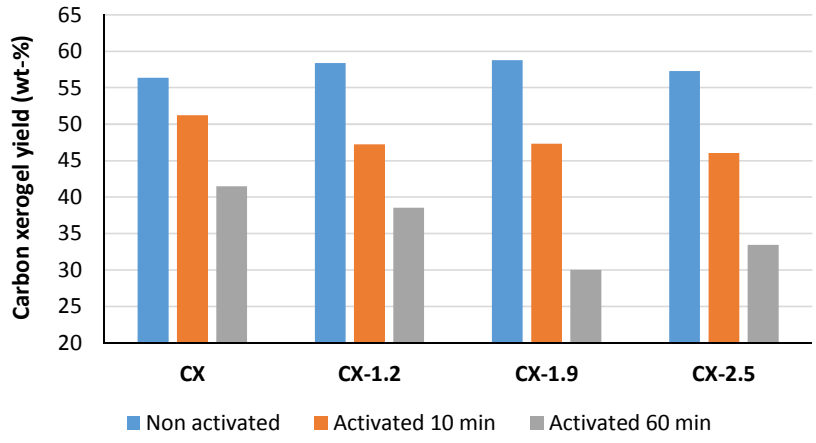


Figure 1. Values of gravimetric yield of carbon xerogels for pristine and GO doped xerogels, when subjected to just carbonization and steam activation during 10 and 60 minutes.

Figure 2 shows the 77 K nitrogen adsorption isotherms of non-activated carbon xerogels. All of them present similar micropore development according to the knee visible at low relative pressures. The pristine carbon xerogel presents a type IV isotherm with a clear hysteresis loop at high relative pressure, indicating the presence of medium size mesopores. The addition of GO produces the disappearance of the hysteresis loop and a big increase of nitrogen adsorption at saturation conditions, which means that the presence of GO produces a carbon gel with a big contribution of large mesopores-macropores, which means that the presence of GO produce the net effect of of the widening of medium-size mesopores into large mesopores-macropores. This latter fact might be due a higher presence of acid groups due to GO surface chemistry. Table 1 shows the porous properties calculated from adsorption isotherms for non-activated samples. Pristine xerogel attains a BET surface area of 760 $m^2/g$, whereas GO containing xerogels develop less surface area, the higher the GO content, the lower the surface area. The average micropore size becomes also smaller due the incorporation of GO. As a consequence, the presence of GO yields lower surface area and widens the mesopores into high sized mesopores/macropores.It is also noticeably that total pore volume begins to decrease at the highest GO content studied.

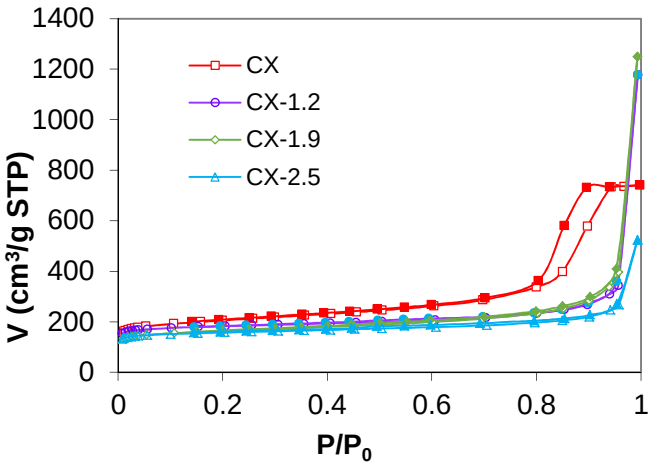


Figure 2. 77 K nitrogen adsorption isotherms of the series of undoped and doped carbon xerogels with different amount of GO.

Table 1. Porous properties of non-activated doped-carbon xerogels, obtained from 77K $N_2$ adsorption isotherm data.

| Sample | 77K nitrogen adsorption isotherm parameters | | | |
|---|---|---|---|---|
| | $S_{BET}$ ($m^2/g$) | $V_{micro}$ ($cm^3/g$) | $L_o$ (nm) | $V_p$ ($cm^3/g$) |
| CX | 760 | 0.30 | 1.2 | 1.14 |
| CX-1.2 | 710 | 0.28 | 0.9 | 1.82 |
| CX-1.9 | 620 | 0.24 | 1.1 | 1.93 |
| CX-2.5 | 614 | 0.24 | 0.9 | 0.81 |

In the case of steam activated samples, nitrogen adsorption isotherms retain the same shape as the parent carbonized samples but with a higher amount adsorbed at low relative pressure. The surface area values increase for all the samples with a corresponding high increase in the micropore volumes, and also a moderate increment in the total pore volumes (see SD). Figure 3 shows the evolution of the BET specific surface area versus burn-off (weight loss upon activation on a percentage basis). As expected, the BET surface area increases with burn-off for all the samples. The pristine activated xerogels, although less reactive with steam, show a slightly greater pore development tendency than the GO doped activated samples. The latter samples exhibit a lower tendency in the pore development due to two possible reasons: a) the lower surface area and micropore volume of the parent GO doped carbonized xerogels than those of the pristine one, or b) the high steam gasification rate produces more external burning (and less micropores) than the low reaction kinetics. In any case, graphene xerogels with excellent surface areas above 1700 $m^2/g$ were obtained.

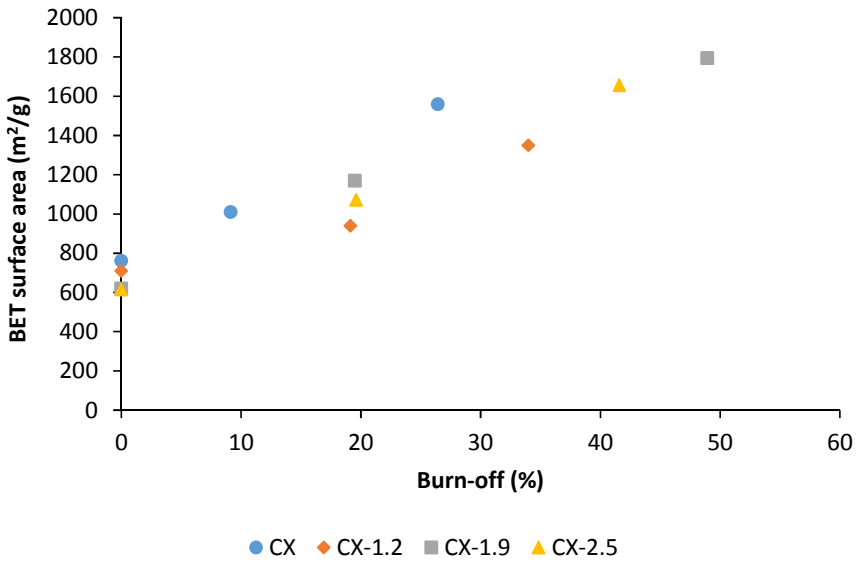


Figure 3. BET specific surface area versus activation burn-off plotted for pristine and GO doped activated xerogels

Figure 4 shows, as example, the CV plots obtained for representative carbonized and activated samples at 1, 5, 50 and 500 mV/s. Figure 4.a and 4.b show CV plots for CX and ACX-60, respectively, and Figure 4.c and 4.d. show the corresponding CVs for CX-1.9 and ACX-1.9-60. Although some CV experimental data present high baseline noise, especially at low scan rates, it can be observed that there is no sign of pseudocapacitance behavior and therefore all the capacitance must be attributed to double layer electrochemical storage. An apparently exception to this seems to be sample ACX-60 at mV/s. However, fluctuation in the upper branch of the cycle should be attributed to an anomaly in the experiment rather than to a pseudocapacitance, since cycles at higher scan rates, carried out on the same sample, do not show any sign of pseudocapacitance. It must be taking into account that the CVs of each sample at different scan rates (20 cycles at each specific scan rate) were carried out with the same electrode samples, starting by the lowest scan rate and then increasing. As a consequence, 500 mV/s was run at the end, and clearly does not present any pseudocapacitance. With respect to pristine carbonized and activated xerogels, the specific capacitances decrease considerably with increasing scan rate as expected,. and higher values of capacitance were obtained for the activated equivalent samples (except at 500 mV). On the other hand, this does not happen with the GO doped CX-1.9 derived samples, where the carbonized sample CX-1.9 (600 $m^2/g$) shows better and more stable

values than a highly activated CX-1.9-60 (1800 $m^2/g$), which displays a deep decay of its properties when increasing scan rate. Similar results were obtained for CD cycles for the same samples, shown in SD for 1 A/g.

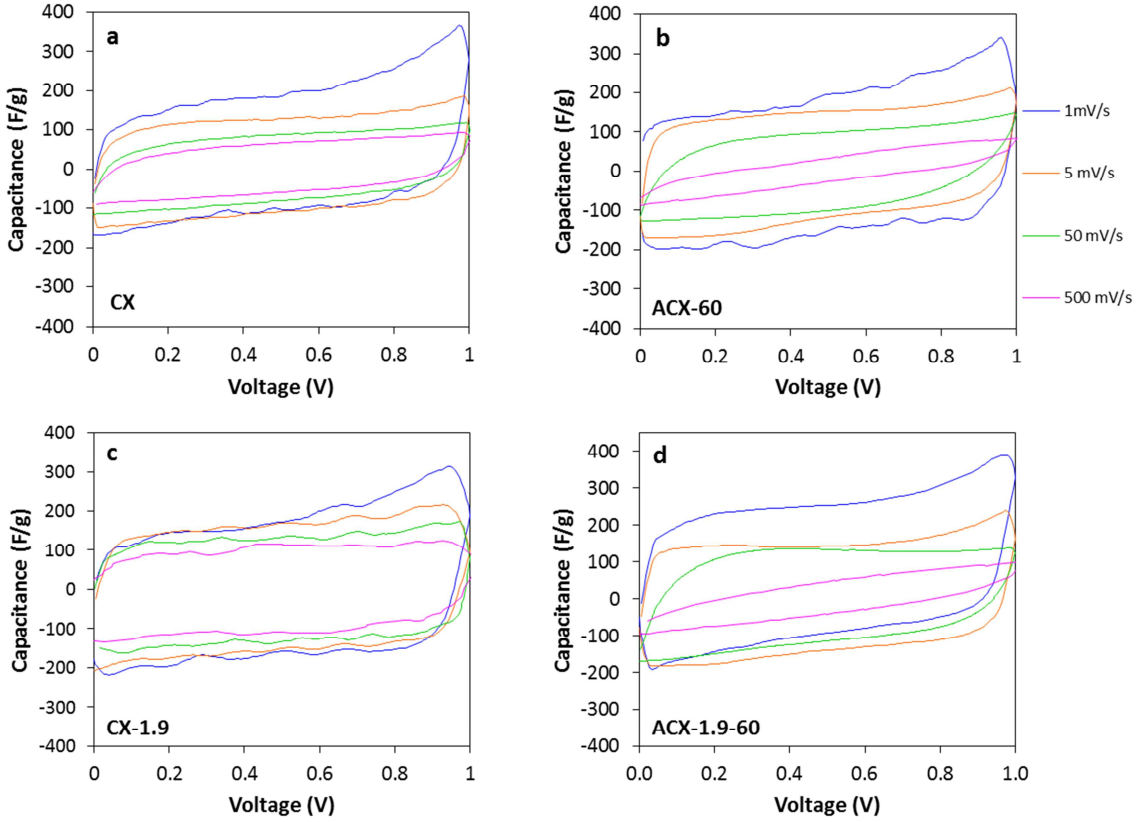


Figure 4. CV plots for carbonized and activated samples at 1, 5, 50, 500 mV/s. Figure 4.a, 4.b CV plots for CX and ACX-60, respectively, and Figure 4.c, and 4.d. CVs for CX-1.9 and ACX-1.9-60.

Figure 5 shows the specific capacitances, calculated from the CVs, for all the non-activated and activated carbon xerogels (GO doped or pristine), versus the scan rates, with range from 1 mV/s to 500 mV/s (Figures 5.a, 5.b, 5.c and 5.d show the results for CX, CX-1.2, CX-1.9 and CX-2.5 derived samples, respectively). Generally, the activated xerogels show a higher capacitance than their corresponding parent carbonized ones at 1 mV/s, as expected. Nevertheless, two different tendencies can be observed at higher scan rates. The undoped samples show a decrease in their performance in a similar extent when the scan rate is increased, presenting a higher decrease rate the ACX-60 at high scan rates, indicative of severe electrolyte ions diffusion at those conditions. However, the second tendency corresponds with low and medium GO content xerogels. Carbonized CX-1.2 and the CX-1.9 xerogels present much more

stable capacitances that their corresponding activated samples, to the point that their performance is much better in the case of the carbonized samples, above 125 F/g with only 600 $m^2$/g, than for the activated samples, 45 F/g with 1800 $m^2$/g, at 500 mV/s. The highly activated ACX-1.2-60 and ACX-1.9-60 samples show a sharp decrease in performance above 100 mV/s, indicating that the GO doped non-activated and the slightly activated xerogels have a key property that enhances their performance even though their BET surface area is lower. The xerogels with the higher GO content display a different trend, since the non-activated sample always shows a slightly lower capacitance than the activated samples, and highly activated ACX-2.5-60 does not undergo a very sharp decrease in capacitance at scan rates above 100 mV/s. It is the non-activated CX-1.2 and CX -1.9 samples that show the best capacitance results, around 120 F/g at 500 mV/s, which represents a decrease in capacitance of only 24% with respect to the value at 1 mV/s, when it can exceed 65% in the case of the pristine sample. These results are of great importance, since capacitors must supply the greatest amount of power as possible, and non-activated samples are much more economic due to their considerably higher yield.

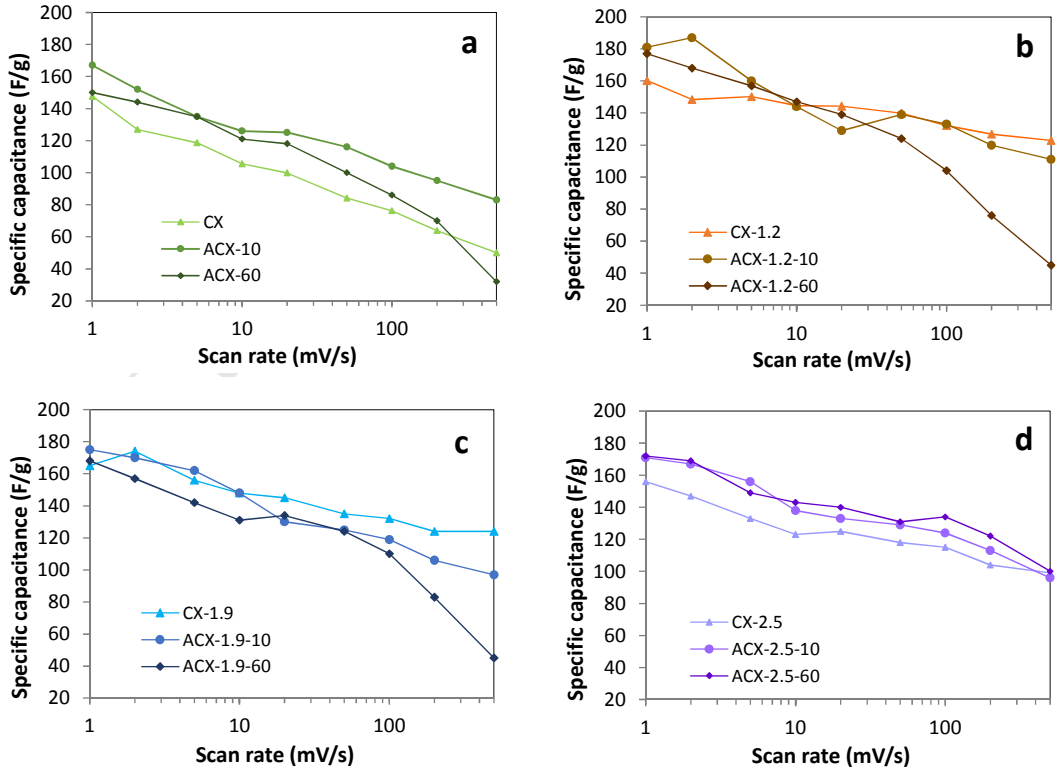


Figure 5. Specific capacitance, calculated from CV, of the activated carbon xerogel CX (a), CX-1.2 (b), CX-1.9 (c) and CX-2.5 (d), at different activation times (10 minutes and

1 hour), at different scan rates compared to that the corresponding non-activated samples.

Figure 6 shows the variation of the specific capacitances of carbonized xerogels calculated from the charge/discharge (CD) cycles versus their working current densities, from 0.1 to 1 A/g (per gram of one electrode). The specific capacitances of all the GO carbonized carbon xerogels are very similar and stable with increasing current density, and much greater than the specific capacitance of the pristine carbonized xerogel, with much clearer differences with respect to the values obtained from CV. The capacitances of the GO doped xerogels are in between 135-160 F/g, whereas the pristine xerogel shows much lower values (between 65 and 105 F/g) and more marked decay with increasing current density. In this case, the capacitance at 1 A/g is only 59% of that obtained at 0.1 A/g, whereas around 85% of the capacitance is retained in the GO containing xerogels. In addition, very similar capacitance values are obtained for the activated and non-activated doped xerogels (see SD), regardless of their BET surface area. This is not the case for the capacitances measured from the CD cycles of activated pristine xerogels, which show higher values with increasing BET surface area.

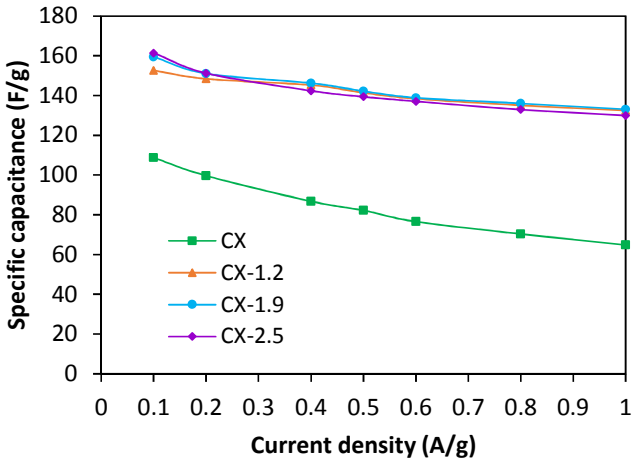


Figure 6. Specific capacitance, calculated from CD cycles, as a function of current density with U=1V of the catbonized carbon xerogel with different amount of GO.

Figure 7 shows the Ragone plot, calculated from the CD at 1 A/g, for all the samples, with different amounts of GO and without any GO (with different symbols for each), and non-activated and activated samples (solid and clear, respectively). The best performance, in terms of high energy and power density, corresponds very clearly to

GO non-activated xerogels, especially those with 1.2% and 1.9% in the parent organic gels. These samples, with less than 700 $m^2/g$, nearly double the performance of the equivalent non-activated pristine xerogel in terms of both energy and power density. The large difference in power density is due to big differences in ESR which are much lower in the carbonized GO-doped xerogels than in the pristine ones. With respect to the performance of GO-doped activated xerogels, it is close to, but slightly lower than that of the graphene doped non-activated xerogels, with an intermediate ESR. Consequently, ESR seems to play more important role than the BET specific surface area. This parameter is known to depend greatly on the electrical conductivity of the materials, and it has a relevant repercussion on the power density of the final supercapacitors [38]. In contrast, the non-activated xerogel with the higher GO content, CX-2.5, shows a lower performance than the other non-activated or activated xerogels with smaller GO contents. This indicates that to a better performance is not directly related to the GO content. Rather, it seems that there is an intermediate GO content that facilitates the dispersion of GO sheets over the amorphous carbon matrix, and in turn, a more adequate surface texture. The possibility of introducing GO agglomerates into the carbon matrix increases with the GO content. Very similar results, and consequently derived conclusions, are observed from Ragone plots calculated at charge current density rates of 0.1, 0.2 and 0.5 A/g, as can be found in SD.

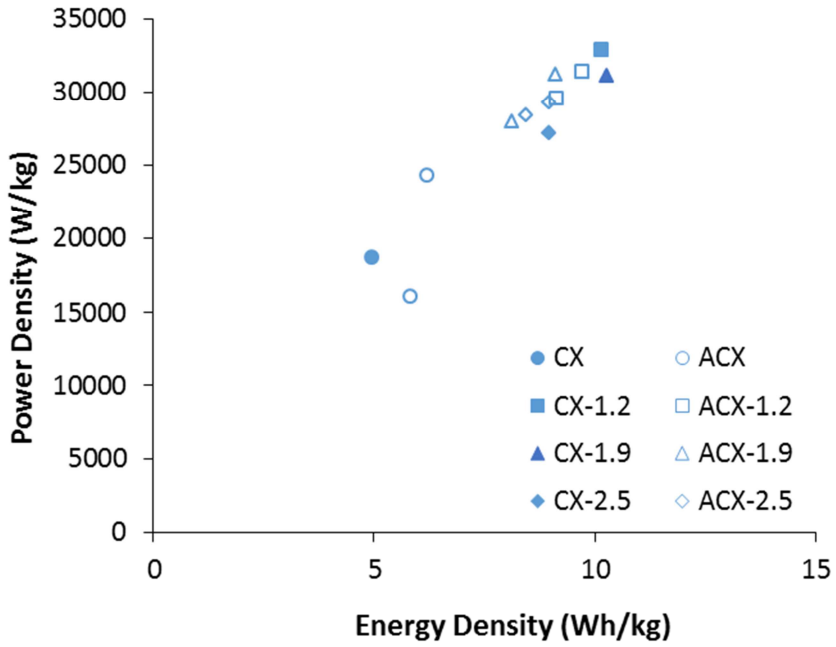

Figure 7. Ragone plot, calculated from CD cycles, for all pristine and GO doped carbon xerogels from CD cycles at 1 A/g.

To clarify the singular results obtained for carbonized GO-carbon xerogel composites, electrochemical impedance spectroscopy (EIS) were performed for selective samples, CX-1.9 and ACX-1.9-60, a carbonized and an activated GO-xerogel composites that present, respectively, the best performance in terms of CV at 500 mV/s and Ragone plot, and a sensible reduction performance that its parent carbonized xerogel. Figure 8 shows the Nyquist plot. First aspect to consider is that the ESR (equivalent series resistance), determined from the first point which intercepts the real axis, is almost the same in both samples (0.08 Ω cm2 for ACX-1.9-60 and 0.1 Ω cm2 for CX-1.9). In addition, none of the samples show a noticeably 45° Warburg Zone. The EDR (equivalent distributed resistance), which is related with the Warburg zone, was determined from the linear projection of the vertical portion at low frequencies to the real axis [39], attaining values of only 0.6 ohm·$cm^2$ for ACX-1.9-6 and 0.9 ohm·$cm^2$ for CX-1.9. That means that the structure of both materials enable the diffusion of the electrolyte ions. Regularly, the resistance decreases at high working frequencies. However, the present materials do not present oxygen content and the cell assembly is the same in both cases, therefore the bigger loop formed at high frequencies in the case of ACX-1.9-60 can be attributed to a higher diffusion resistance.

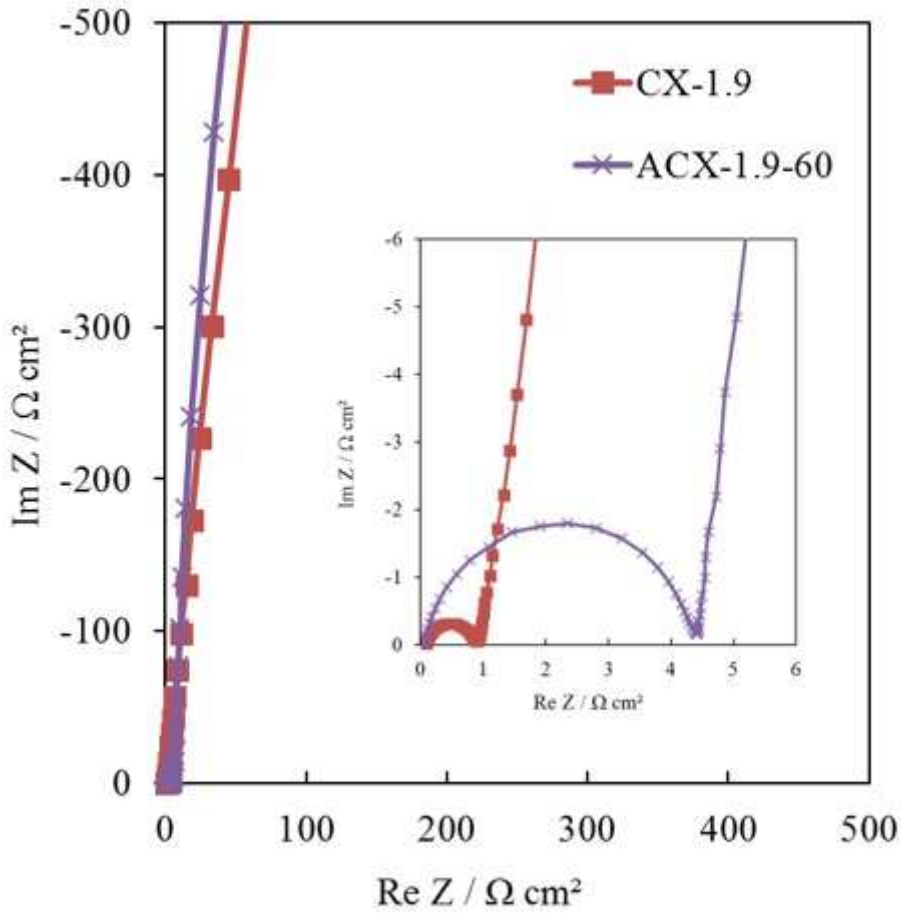


Figure 8. Nyquist plot of CX-1.9 and ACX-1.9-60 (frequency range of 1 mHz-100 kHz) and its magnification at frequency values between 0.193 Hz and 100 kHz.

Finally, the electrical conductivity of all carbon xerogel based electrodes were measured to verify its influence on the performance as a supercapacitor. Figure 9 shows the electrical conductivity for the different carbon xerogels with different contents of GO and activation degrees. Now, there is a clear tendency towards increasing electric conductivity with increasing GO content, especially for non-activated samples, where the conductivity reaches twice the value of the pristine xerogel samples. The conductivity values are also higher than those reported for the amorphous carbon materials typically used in electrochemical applications [6, 12]. Clearly, the increase in electrical conductivity is the factor responsible for the higher values of power density in the GO containing xerogels, as shown in Figure 7. The higher the GO content the higher the conductivity, but an important effect on how this GO is dispersed in the carbon matrix and the final porosity of the composite since, according to Ragone plot, best

performance as a supercapacitor is not obtained at the GO content, i.e. the maximum conductivity.

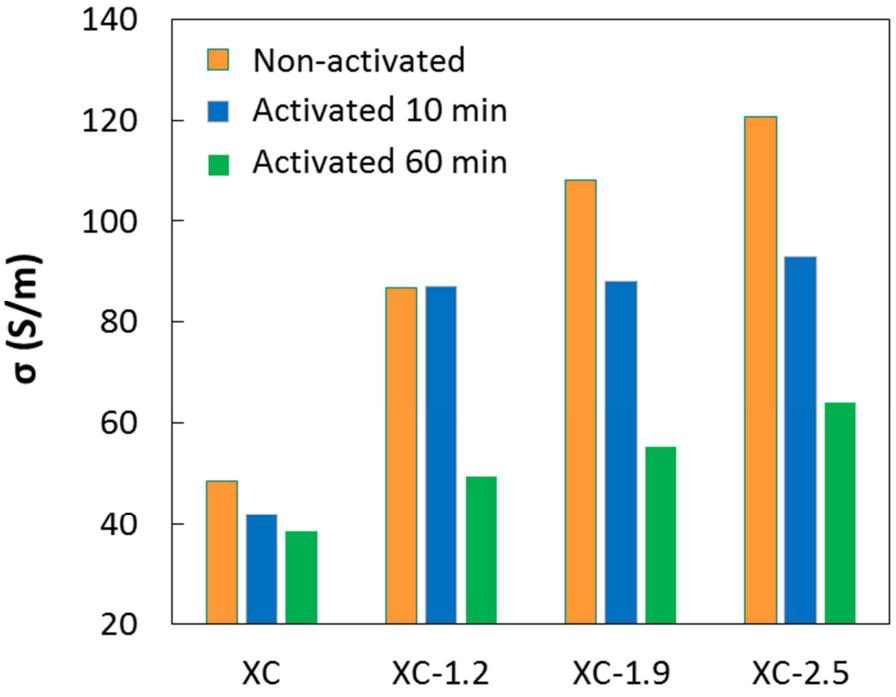


Figure 9. Conductivity of non-activated and activated carbon xerogel based electrodes with different GO contents, calculated by the van der Pauw method.

This could be due to the fact that, during the polymerization process, the GO sheet acts as a scafold for the formation of amorphous gel and the GO sheets are then perfectly distributed throughout the subsequent carbonaceous structure. This enhances the electron mobility and subsequently the electrical conductivity. However, Figure 9 also shows the marked negative effect that steam activation has on the conductivity of xerogel composites, in the form of a drastic decrease, and the higher the activation burn-off, the greater the decrease. In pristine samples, the decrease of conductivity upon activation is not so profound as it is in GO doped xerogels. These results clearly evidence that electrical conductivity plays, in the present samples, a more important role than the BET surface area, which is to our knowledge, the first time this has been confirmed for carbon materials. In addition, the drastic reduction in electrical conductivity upon activation could have occurred for two reasons: activation burns away GO sheets to a greater extent than the amorphous matrix, or simply because the increase in burn-off and pore volume is too large to allow any contact between the

graphene sheets in the amorphous carbon matrix. Both explanations are equally valid, since GO sheets can be considered either imbibed onto the matrix or directly accessible to steam on activation, as can be observed in both TEM and FESEM explorations (see SD). It can be concluded that the incorporation of GO into the non-activated carbon xerogels produces a similar porous texture, with a slight decrease in micropore volume and a relevant widening of medium mesopores into high mesopores-macropores, but the main effect is that GO specially produces a sharp increase in the electrical conductivity of the resulting xerogels.

## 4. Conclusions

- The main conclusion from the present work is that graphene oxide produced a significant enhancement of the electrical conductivity of the carbon xerogel resulting in a marked improvement of both the energy and, especially, power densities, with even better results when carbon xerogels were non-activated and presented only 600 $m^2/g$.
- Electrical conductivity seems to play a more important role than the specific surface area in mesoporous carbon xerogels, since activated GO xerogel composites, with 1000-1500 $m^2/g$ present a lower electrochemical performance, as well as a lower electrical conductivity.
- The optimum amount of GO for optimal performance is low, i.e. below 2 wt-%. Higher GO contents produce lower energy and power densities, although the electrical conductivity continues to show an increasing trend, which means that GO must be individualized and well-dispersed throughout the carbon matrix, with no agglomeration.

**Acknowledgements.**

The authors gratefully acknowledge the financial support of the Ministerio de Economía y Competitividad of Spain, MINECO (Project CTQ2014-54772-P) and CTQ2013-44213-R), and Generalitat Valenciana (project PROMETEOII/2014/007).

**References**

[1] Winter M, Brodd RJ. What are batteries, fuel cells, and supercapacitors? Chem. Rev. 2004;104(10):4245-69.
[2] Armand M, Tarascon JM. Building better batteries. Nat. 2008;451(7179):652-7.
[3] Chu A, Braatz P. Comparison of commercial supercapacitors and high-power lithium-ion batteries for power-assist applications in hybrid electric vehicles: I. Initial characterization. J. Power Sources. 2002;112(1):236-46.
[4] Gamby J, Taberna PL, Simon P, Fauvarque JF, Chesneau M. Studies and characterisations of various activated carbons used for carbon/carbon supercapacitors. J. Power Sources. 2001;101(1):109-16.
[5] Wei L, Yushin G. Nanostructured activated carbons from natural precursors for electrical double layer capacitors. Nano Energy. 2012;1(4):552-65.
[6] Pandolfo AG, Hollenkamp AF. Carbon properties and their role in supercapacitors. J. Power Sources. 2006;157(1):11-27.
[7] Salitra G, Soffer A, Eliad L, Cohen Y, Aurbach D. Carbon electrodes for double-layer capacitors. I. Relations between ion and pore dimensions. J. Electrochem. Soc. 2000;147(7):2486-93.
[8] Kötz R, Carlen M. Principles and applications of electrochemical capacitors. Electrochim. Acta. 2000;45(15-16):2483-98.
[9] Jin Z, Yan X, Yu Y, Zhao G. Sustainable activated carbon fibers from liquefied wood with controllable porosity for high-performance supercapacitors. J. Mater. Chem. A. 2014;2(30):11706-15.
[10] Ania CO, Khomenko V, Raymundo-Piñero E, Parra JB, Béguin F. The large electrochemical capacitance of microporous doped carbon obtained by using a zeolite template. Adv. Funct. Mater. 2007;17(11):1828-36.
[11] Portet C, Yushin G, Gogotsi Y. Electrochemical performance of carbon onions, nanodiamonds, carbon black and multiwalled nanotubes in electrical double layer capacitors. Carbon. 2007;45(13):2511-8.
[12] Wang L, Ding W, Sun Y. The preparation and application of mesoporous materials for energy storage. Mater. Res. Bull. 2016;83:230-49.
[13] Korenblit Y, Rose M, Kockrick E, Borchardt L, Kvit A, Kaskel S, et al. High-rate electrochemical capacitors based on ordered mesoporous silicon carbide-derived carbon. ACS Nano. 2010;4(3):1337-44.
[14] Raymundo-Piñero E, Kierzek K, Machnikowski J, Béguin F. Relationship between the nanoporous texture of activated carbons and their capacitance properties in different electrolytes. Carbon. 2006;44(12):2498-507.
[15] Calvo EG, Lufrano F, Staiti P, Brigandì A, Arenillas A, Menéndez JA. Optimizing the electrochemical performance of aqueous symmetric supercapacitors based on an activated carbon xerogel. J. Power Sources. 2013;241:776-82.
[16] Yang I, Kim SG, Kwon SH, Lee JH, Kim MS, Jung JC. Pore size-controlled carbon aerogels for EDLC electrodes in organic electrolytes. Curr. Appl. Phys. 2016;16(6):665-72.
[17] Goodenough JB. Energy storage materials: A perspective. Energ. Stor. Mat. 2015;1:158-61.
[18] Calvo EG, Ania CO, Zubizarreta L, Menéndez JA, Arenillas A. Exploring new routes in the synthesis of carbon xerogels for their application in electric double-layer capacitors. Energ. Fuel. 2010;24(6):3334-9.
[19] Tsuchiya T, Mori T, Iwamura S, Ogino I, Mukai SR. Binderfree synthesis of high-surface-area carbon electrodes via CO 2 activation of resorcinol-formaldehyde carbon xerogel disks: Analysis of activation process. Carbon. 2014;76:240-9.
[20] Rey-Raap N, Angel Menéndez J, Arenillas A. Simultaneous adjustment of the main chemical variables to fine-tune the porosity of carbon xerogels. Carbon. 2014;78:490-9.
[21] Macías C, Haro M, Parra JB, Rasines G, Ania CO. Carbon black directed synthesis of ultrahigh mesoporous carbon aerogels. Carbon. 2013;63:487-97.

[22] Sepehri S, García BB, Zhang Q, Cao G. Enhanced electrochemical and structural properties of carbon cryogels by surface chemistry alteration with boron and nitrogen. Carbon. 2009;47(6):1436-43.
[23] Zhou Y, Candelaria SL, Liu Q, Huang Y, Uchaker E, CaO G. Sulfur-rich carbon cryogels for supercapacitors with improved conductivity and wettability. J. Mater. Chem. A. 2014;2(22):8472-82.
[24] Fernández PS, Castro EB, Real SG, Visintin A, Arenillas A, Calvo EG, et al. Electrochemical behavior and capacitance properties of carbon xerogel/multiwalled carbon nanotubes composites. J. Solid. State Electrochem. 2012;16(3):1067-76.
[25] Bordjiba T, Mohamedi M, Dao LH. Novel binderless nanostructured carbon nanotubes-carbon aerogel composites for electrochemical double layer capacitors. ECS Transactions; 2008; 2008. p. 183-9.
[26] Xia J, Chen F, Li J, Tao N. Measurement of the quantum capacitance of graphene. Nat Nano. 2009;4(8):505-9.
[27] Dreyer DR, Park S, Bielawski CW, Ruoff RS. The chemistry of graphene oxide. Chem. Soc. Rev. 2010;39(1):228-40.
[28] Lee YJ, Kim G-P, Bang Y, Yi J, Seo JG, Song IK. Activated carbon aerogel containing graphene as electrode material for supercapacitor. Mater. Res. Bull. 2014;50:240-5.
[29] Qian Y, Ismail IM, Stein A. Ultralight, high-surface-area, multifunctional graphene-based aerogels from self-assembly of graphene oxide and resol. Carbon. 2014;68:221-31.
[30] Hummers Jr WS, Offeman RE. Preparation of graphitic oxide. JACS. 1958;80(6):1339.
[31] Pekala RW. Organic aerogels from the polycondensation of resorcinol with formaldehyde. J Mater Sci. 1989;24(9):3221-7.
[32] Brunauer S, Deming LS, Deming WE, Teller E. On a Theory of the van der Waals Adsorption of Gases. JACS. 1940 1940/07/06;62(7):1723-32.
[33] Dubinin MM, Kadlec O. New ways in determination of the parameters of porous structure of microporous carbonaceous adsorbents. Carbon. 1975;13(4):263-5.
[34] Stoeckli HF, Kraehenbuehl F, Ballerini L, De Bernardini S. Recent developments in the Dubinin equation. Carbon. 1989;27(1):125-8.
[35] Van Der Pauw LJ. A method of measuring specific resistivity and hall effect of disks of arbitrary shape. Van Der Pauw, L.J. Phil. Res. Rep. 1958;13: 1-9.
[36] Euler KJ. The conductivity of compressed powders. A review. J. Power Sources. 1978;3(2):117-36.
[37] Celzard A, Marêché JF, Payot F, Furdin G. Electrical conductivity of carbonaceous powders. Carbon. 2002;40(15):2801-15.
[38] Ling Z, Wang G, Dong Q, Qian B, Zhang M, Li C, et al. An ionic liquid template approach to graphene-carbon xerogel composites for supercapacitors with enhanced performance. J. Mater. Chem. A. 2014;2(35):14329-33.
[39] Sevilla M, Yu L, Ania CO, Titirici MM. Supercapacitive behavior of two glucose-derived microporous carbons: direct pyrolysis versus hydrothermal carbonization. ChemElectroChem 2014; 1:2138-2145.